Electronic excitations in $PrAlO_3$

K. B. Lyons, R. J. Birgeneau, E. I. Blount, and L. G. Van Uitert
Bell Laboratories, Murray Hill, New Jersey 07974
(Received 23 September 1974)

Previous spectroscopic experiments have shown that $PrAlO_3$ exhibits structural phase transitions at ~ 1640, 205, and 151 K from respectively cubic to rhombohedral to orthorhombic to monoclinic symmetry. The 205 and 151 K transitions are now known to be driven by the coupling between the low-lying Pr^{3+} electronic levels and the phonon modes corresponding to staggered rotations of the AlO_6^{3-} octahedra. In this paper we report an electronic Raman spectroscopic investigation of the crystal-field excitons originating in transitions from the ground and first excited states of the Pr^{3+} atom to the uppermost (A_1) level of the Pr^{3+} $^3H_4$ ground manifold. The principal results of this study are (a) the over-all splitting of the $^3H_4$ manifold varies markedly with temperature, ranging from ~ 750 cm^{-1} at 300 K to 925 cm^{-1} at 20 K. (b) Thermally induced two-exciton Raman scattering is observed in the orthorhombic and monoclinic phases; the ground-state–first-excited-state splittings so determined are in good agreement with the corresponding fluorescence results. (c) In the orthorhombic phase the Raman selection rules imply that the ground state is $B_1(C_{2v})$ rather than $A_1(C_{2v})$ as previously supposed. Results (a) and (c) are in substantial numerical disagreement with the recent model calculation of Birgeneau *et al.* We have extended this calculation to include the effect of the $^3H_5$ manifold. This more quantitative crystal-field analysis yields a good description of all measured levels at all temperatures with (in the notation of Birgeneau *et al.*) $B_2 = 825$, $B_4 = -699$ cm^{-1}, $B_6 = -949$ cm^{-1}, and $\alpha = 0.4$. The standard deviation of the fit in the orthorhombic phase and at $T \sim 0$ K is 27 cm^{-1}, which is the limit of the accuracy of the calculation.

I. INTRODUCTION

The perovskite $PrAlO_3$ is known[1,2] to undergo a series of structural phase transitions at 1640, 205, and 151 K. A fourth transition at 118 K has recently been discovered.[3] It has been shown[1,2] that the 151- and 205-K transitions occur as a result of a delicate interplay between anharmonic and electronic contributions to the crystal energy. The electronic contribution comes about from the dependence of the crystal-field levels on the structural deformation of the crystal. In particular, the crystal can lower its total energy by undergoing a distortion which causes an increase in the splitting of the ground doublet of the $2f^2\,^3H_4$ manifold, decreasing the electronic energy at the expense of a smaller increase in the elastic energy. Such a transition, caused by the linear electron-phonon interaction, is known as a cooperative Jahn-Teller transition and has been discussed extensively elsewhere.[2,4]

While the effect of the lattice deformation on the low-lying states is most important for understanding the phase transitions, the lattice deformation affects all the crystal-field levels of the Pr^{3+} ion. A valid theory of the transitions should describe properly the behavior of all the levels. A model for such behavior was proposed,[1] and the accompanying calculations gave a reasonable description of the existing data.

There was then, however, no information on the total width of the $J = 4$ manifold. The work described in this paper was undertaken to obtain this information. The width was measured by Raman spectroscopy from 20 K to room temperature. An additional Raman line was observed in the same region, which we attribute to the transition of an exciton from the lowest excited state to the highest state of the $J = 4$ manifold. Finally, in light of the new data and their poor agreement with existing calculations, we have refined the crystal-field calculation and now find good agreement with the data. The standard deviation of 27 cm^{-1} is as good as could be expected from the simple model and calculation.

The background of this work, both experimental and theoretical, is described more fully in Sec. II. The experimental results are discussed in Sec. III. The extension of the calculation and discussion of the data are given in Sec. IV.

II. EXPERIMENTAL AND THEORETICAL BACKGROUND

Experimentally it has been found[1,5] that the distortions involved in the structural phase transitions may be simply described as staggered rotations of the AlO_6^{3-} octahedra. The axis of that rotation changes with temperature while the amount of rotation remains relatively constant (9.4°). This rotation causes a doubling of the unit cell in the (111) direction, regardless of the direction of the axis of rotation. The cubic perovskite structure exists above 1320 K. Between 210 and 1320 K, in the rhombohedral phase, the axis of rotation is the

(111) direction in the perovskite lattice. Between 151 and 210 K the axis is in a perovskite (101) direction, resulting in orthorhomic symmetry. Below 151 K the axis moves continuously from the (101) direction toward (001) or (100). This reduces the symmetry to monoclinic, but at low temperature it becomes approximately tetragonal. According to this model the two Pr^{3+} sites in the unit cell are always related by inversion; that is, lattice-inversion symmetry about the Al sites is never lost. These rotations of the aluminate octahedra are shown diagrammatically in Fig. 1 for clarity. There is an additional small macroscopic strain which changes from one phase to another. The main distortion results from the rotation of the aluminate groups.

The material has been studied by a variety of techniques, including Raman and fluorescence spectroscopy,[2] neutron scattering,[1] ESR,[5] specific heat,[6] and x-ray crystallography.[7] All of these prior results appear to be explained by the crystallographic description given above and theoretical treatments stemming from that description.[1,2] A simple crystal-field model for the electronic levels in $PrAlO_3$ has been proposed by Birgeneau *et al.*[1] Since this model will be the basis for all our calculations in this paper we describe it in detail here. Quite generally, the crystalline-electric-field (CEF) potential may be written

$$\mathcal{H}_{\mathrm{CEF}} = \sum_{\substack{n=2,4,6 \\ m=-n,n}} B_n^m \chi_n \tilde{O}_n^m , \tag{1}$$

where the $\tilde{O}_n^m$ are normalized angular-momentum operators, the χ_n are reduced matrix elements, and the B_n^m are the CEF coefficients. In cubic symmetry the only CEF coefficients are $B_4 = B_4$, $B_4^{\pm 4} = (\frac{5}{14})^{1/2} B_4$, $B_6 = B_6$, $B_6^{\pm 4} = -(\frac{7}{2})^{1/2} B_6$. The essential assumption of the CEF model of Birgeneau *et al.* is that in the distorted aluminate phases B_4^m, B_6^m retain those values appropriate to the ideal cube perovskite structure. The distortion then manifests itself only in the B_2^m field-gradient terms, which are quadratic in the over-all angle of rotation. As discussed in the Appendix, it can be shown quite generally that for a staggered rotation of the AlO_6^{3-} octahedra about an axis with direction cosines $(\cos\theta_x, \cos\theta_y, \cos\theta_z)$ the field-gradient tensor has the form

$$\begin{aligned} B_{ii} &= B_2(3\cos^2\theta_i - 1), \\ B_{ij} &= -3B_2\alpha\cos\theta_i\cos\theta_j, \\ i,j &= x, y, z. \end{aligned} \tag{2}$$

The corresponding expressions for the B_2^m are immediately derivable from Eq. (2) using the appropriate definitions of the $\tilde{O}_2^m$. This model thus reduces the total number of CEF parameters from, for example, 15 for the monoclinic phase to the four fundamental parameters B_2, α, B_4, and B_6. These four parameters should apply in all phases provided that the over-all rotation angle Q is fixed ($B_2 \sim Q^2$).

It is also expected that B_2, B_4, B_6 will vary smoothly from one rare-earth aluminate to another. As we shall discuss later, these parameters have in fact been determined for $NdAlO_3$, so a test of this expectation is possible. Finally, the factor α determining the relative sizes of the E_g and T_{2g} components of the field-gradient tensor $\overleftrightarrow{B}$ may be calculated on a point-charge model (PCM). As discussed in the Appendix, if one includes just the rotations of the AlO_6^{3-} octahedra then the PCM gives $\alpha = \frac{2}{3}$. The strain contributions are rather more complicated and depend in detail on the coupling constants relating the strain to the rotation. Thus α may be taken as an adjustable parameter to be determined by experiment.

Birgeneau *et al.* have applied this model to the various phases of $PrAlO_3$, considering only the ground $^3H_4$ manifold. The results, which are shown in Fig. 2, agreed with the then-available data within the accuracy of the calculation (estimated to be ~ 100 cm^{-1}).

As shown also in Fig. 2, our new experimental results deviate significantly from the results of the simple model described above. The main source of the 100-cm^{-1} error estimate above is the neglect of the effect of the higher multiplets, in particular the $^3H_5$, which is separated from the $^3H_4$ manifold by only 2100 cm^{-1}. The calculations described in Sec. IV include this effect, and we find that the model is then capable of quantitative agreement with all of the available data within the expected accuracy of about 25 cm^{-1}.

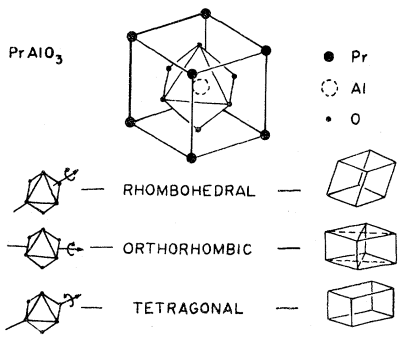

FIG. 1. Distortion of the perovskite unit cell in $PrAlO_3$, shown as rotation axes for the aluminate octahedra.

III. EXPERIMENTAL PROCEDURE AND RESULTS

The calculations of Birgeneau *et al.* described above predict a value for the total width of the $J = 4$ manifold, which is the separation of the lower and

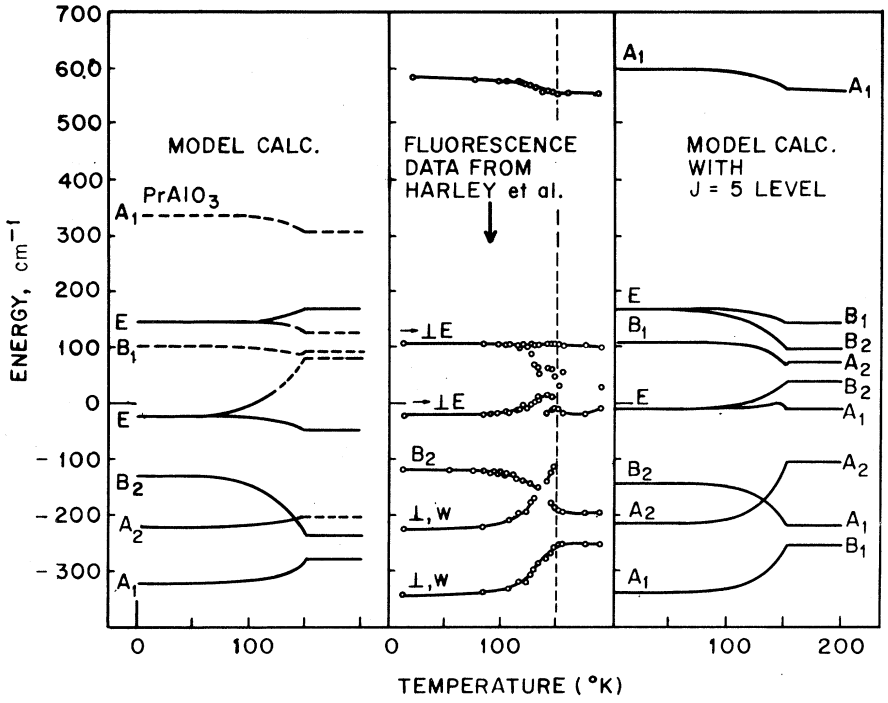

FIG. 2. Comparison of theory to data. On the left-hand side is the previous crystal-field calculation. In the center are the data (fluorescence and Raman). On the right-hand side are the results of the extended crystal-field calculation.

higher A_1 levels, of about 700 ± 100 cm^{-1} at low temperatures. Since this excitation should be Raman active it was decided to investigate it via Raman scattering.

The data were taken with a single crystal of $PrAlO_3$ with natural faces perpendicular to the perovskite axes. The incident light was 5145-Å Ar^+ laser radiation. Only 10 mW of power were used in the vicinity of the transition to avoid significant heating effects. The crystal was mounted on a cold finger cooled by flowing He gas for temperature control which was good to ± 0.04 °K. The laser heating in the sample volume was probably no more than 0.2 °K. The scattered light, collected by $f/4$ optics, was analyzed by a Spex 1401 double monochromator and an EMI 62565 phototube cooled by LN_2 was used as a detector.

The pattern displayed by the transmitted laser beam turned out to be a good indicator not only for the phase transitions but also for the domain character of the sample. On passing the first-order transition (~208 K) the previously "clean" transmitted beam disappeared and was replaced by a diffuse smear, apparently produced by scattering from microdomains. This situation persisted down to about 100 K, where the crystal cleared dramatically, producing a transmitted pattern consisting of one or a few bright spots. The exact pattern depended on the position of the beam in the sample, indicating the presence of several large domains in our crystal. The data analyzed were taken with the scattering volume apparently contained in a single domain. Once this "clearing" had occurred the sample could be heated up to, but not through, the first-order transition without returning to the microdomain state. The data taken in the microdomain state did *not always* agree with that taken in the cleared state. This can be seen in Fig. 3, where spectra taken in the microdomain and cleared states of the same crystal are displayed (spectra a and b).

In a different domain of the cleared crystal we observed both lines with the same frequencies as in the microdomain state, but we never observed the uppermost line alone. This situation persisted down to about 145 K (i.e., well into the monoclinic phase) where these "selection rules" began to break down. The next three spectra (c, d, e) serve to illustrate the situation. As the temperature was lowered further the lower line weakened and disappeared at about 110 K, leaving only the upper line (spectrum f). The temperature dependence of the frequencies of the two lines is shown in Fig. 4. Lines were observed in diagonal Raman polarizations (xx, yy, or zz referred to perovskite axes) but were not present in off-diagonal polarizations (xy, etc.).

The simplest interpretation of this pair of lines is that they represent transitions to the upper A_1 level from the states originating in the ground doublet of the rhombohedral phase. Since the splitting of the latter states is known from fluorescence measurements as well as other Raman-scattering data, it is easy to check this idea, as shown in

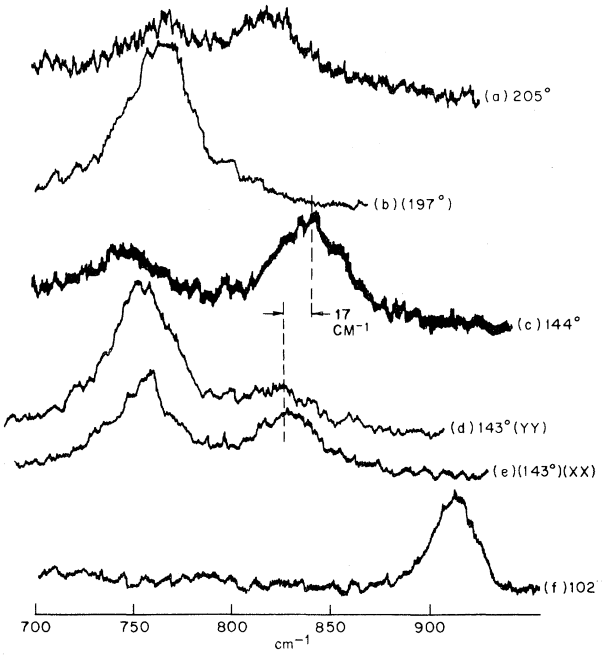

FIG. 3. Typical Raman spectra of the upper A_1 $^3H_4$ level. All represent diagonal Raman tensor elements. (a) Orthorhombic phase, microdomain. (b) Orthorhombic, monodomain. Absence of upper line indicates *yy* geometry. (c) Monoclinic phase, microdomain. (d) and (e) Monoclinic single domain with different orientations. The *yy* orientation is defined as that in which spectrum b was taken (see text). (f) Low temperature (nearly tetragonal), geometry no longer has an effect.

Fig. 5. The transition from the excited state to the upper level is a two-exciton process in that it involves destruction of one exciton and creation of another. It is interesting to note that the ob-

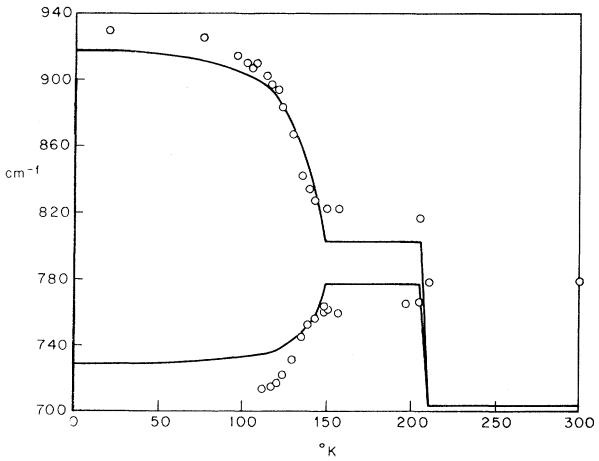

FIG. 4. Temperature dependence of the lines observed near the upper A_1 level. The data are shown as circles and the solid line is the result of the crystal-field calculation described in the text.

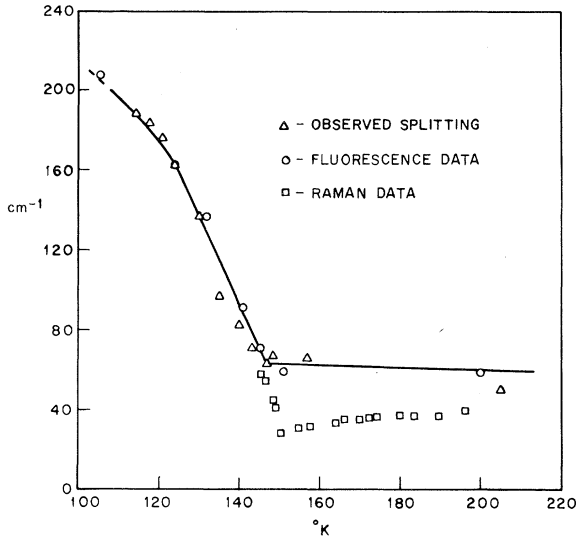

FIG. 5. Splitting between the two lines observed as a function of temperature, plotted with the fluorescence and Raman data from (Harley *et al.*) for the splitting of the ground doublet. The solid line is a guide to the eye.

served splitting agrees better with the fluorescence results than with the Raman results, as expected for a two-exciton process, since the orthorhombic B_1 exciton is known to have appreciable dispersion (Fig. 5).

This interpretation is supported by the selection rules. The ground doublet of the rhombohedral state splits into A_1 and B_1 states in the orthorhombic phase. Referred to perovskite axes, the A_1-A_1 transition should be active in *xx*, *yy*, and *zz*, and thus be observed in all domains. However, if the axis of rotation is (101) the B_1-A_1 should be active in *xx* and *zz* polarizations but not in *yy*. Although we were unable to orient our sample magnetically, it seems reasonable to conclude that the line which is always present represents the A_1-A_1 and the one sometimes present represents the B_1-A_1 transition. An alternative explanation, which we consider improbable, is that all of our data were accidentally taken in *xx* or *zz* (never *yy*) and that one diagonal element for the A_1-A_1 transition is accidentally small. The former explanation leads to the conclusion that the ground state in the orthorhombic phase is the B_1. This is in apparent conflict with the previous calculations,[1] but it will be shown in Sec. IV that this discrepancy is removed by our perturbation calculation.

The fact that the upper line strengthens and dominates at lower temperatures is also understandable on this basis. In the monoclinic phase, the states derived from the A_1 and B_1 states of the orthorhombic phase both transform according to the same representation and, as will be seen in

Sec. IV, the B_1 (C_{2v}) (ground) state of the orthorhombic phase evolves in the tetragonal limit into an A_1 (D_{2d}) level and the A_1 (C_{2v}) into a B_2 (D_{2d}) level. The former should be active in xx, yy, and zz, as it is. The fact that the B_2 is inactive in all these polarizations, while true, has little importance since the state is thermally depopulated by about 110 K, so that the line would disappear in any event.

One last comment is in order concerning the discrepancy between the positions of the upper line in spectra c and d of Fig. 2. Among the possible explanations for this are (i) The line in spectrum d could be a Davidov-split line due to the additional doubling of the unit cell (requiring breaking of inversion symmetry[8]); (ii) a phonon-assisted transition; or (iii) an impurity-shifted excitation. The most likely explanation, however, is simply that it is the same line as in spectrum c, shifted by strains caused by the existence of many small domains. Since the domains have significantly different lattice parameters for a given direction, such strains are unavoidable. The fact that on recycling the crystal developed microcracks and eventually disintegrated is also indicative. This explanation is consistent with the fact that the line in spectrum c overlaps that in d. Since the upper level is strongly coupled to the strain, as is evident from the crystal-field calculations, it is not surprising that such internal strains would lead to an appreciable shift. We are not, however, in a position to make this argument quantitative.

The fact that the splitting of the pair of lines agrees with the fluorescence data indicates that the zone-center energy of the upper A_1 state is virtually the same as the zone-average value, since the latter is measured by the two-exciton process. Since the dispersion of the $^3P_0$ state (from which the fluorescence was measured) should be small, we conclude that that of the upper A_1 level should be similarly small.

IV. CALCULATIONS

The results described above show discrepancies with the previous calculations. The most obvious is that the total splitting observed (925 cm^{-1}) is over 150 cm^{-1} larger than previously. Further, when only the $J=4$ manifold is considered with the potential used in Eq. (1) it is known that the ratio of the A_1-A_1 splitting to the A_1-(upper) E splitting (in the tetragonal phase) is $\sim\frac{7}{5}$.[9] The observed ratio is 1.8, 30% larger. In addition the selection rules indicate that the ground-state symmetry in the orthorhombic phase is probably B_1 (C_{2v}) rather than A_1 (C_{2v}).

In an effort to clear up these discrepancies, the calculation mentioned in Sec. II was extended to include second-order perturbative effects of the $J=5$ manifold. The necessary reduced matrix elements for this calculation have been tabulated by Abragam and Bleaney.[10] The $J=5$ manifold was treated as though it were unsplit for this calculation. The errors introduced by this approximation should be less than one-fifth of the shifts, i.e., less than 20 cm^{-1}. Let us represent the atomic states by the states $|JM_J\rangle$. Diagonalization of this Hamiltonian [Eq. (1)] within the $^3H_4$ manifold yields the states

$$|\psi_J^i\rangle = \sum_{M_J=-J}^{J} \alpha_{M_J}^i |JM_J\rangle, \tag{3}$$

with energies E_i.

We then calculate the matrix elements [see Eq. (1)]

$$\langle 5M | \mathcal{H}_{\mathrm{CEF}} | \psi_J^i \rangle = R_{iM} \tag{4}$$

by standard techniques, and the perturbation of the Hamiltonian for the $J=4$ manifold is given by

$$\Delta H_{ij} = -\sum_{M=-5}^{5} \frac{|R_{iM}R_{Mj}|}{2}\left(\frac{1}{E-E_i}+\frac{1}{E-E_j}\right), \tag{5}$$

where $E=2100$ cm^{-1} is the splitting of the $J=5$ manifold from the $J=4$. The resulting Hamiltonian matrix was then diagonalized again within the $J=4$ manifold. Using the low-temperature data we fitted this model by an iterative least-squares approach, varying B_2, B_4, and B_6. The best fit gave a standard deviation of 25 cm^{-1} (Table I). The parameter α was then chosen by a least-squares fit to the eight known levels in the orthorhombic phase,[11] together with the total width of the manifold in the rhombohedral phase, as shown in Table I. This gave a value of 0.4 ± 0.1 for α. An alternate fitting procedure,[12] using the orthorhombic data to determine all four parameters, yielded similar parameters. These results of the former fit were shown in Fig. 2. The reader will note that the agreement for the single data point in the room-temperature phase (D_3) is poorer (9%). This is not surprising since B_2, B_4, B_6 were determined from data taken at ~0 K. However, the fit in the orthorhombic phase is well within the expected uncertainties in both the data and the calculation. In particular, the total width of the manifold is now adequately explained by the model and the ground state is of B_1 (C_{2v}) symmetry. Furthermore, we can now interpret the rather puzzling fluorescence data of Harley *et al.* in the region 125–150 K between the E levels as the result of interaction between states derived from the B_2 and A_2 states of the orthorhombic phase. In addition, the crystal-field parameters found in the least-squares fit are within 8% of the parameters for $NdAlO_3$.[10] The remaining discrepancies of ~25 cm^{-1} (rms) may be

TABLE I. Comparison of experimental and calculated line positions. All values in cm^{-1}.

	Level symmetry	E_{expt} [a]	E_{calc} (D_{2d} fit)	E_{calc} (C_{2v} fit)
Tetragonal phase	A_1	(0)	(0)	(0)
	A_2	117	117	138
	B_2	224	188	146
	E	319	319	300
	B_1	(?)	445	394
	E	445	493	444
	A_1	925	916	899
Orthorhombic	B_1	(0)	(0)	(0)
	A_1	57	35	36
	A_2	(160)	144	171
	A_1	238	235	240
	B_2	282	282	271
	A_2	(?)	318	322
	B_2	311	341	306
	B_1	357	388	365
	A_1	821	801	817
Rhombohedral	A_1	778	695	712
Total standard deviation			31 cm^{-1}	30 cm^{-1}
CEF parameters	α	($NdAlO_3$)	0.4 ± 0.1	0.36 ± 0.1
	B_2	795	825 ± 86 cm^{-1}	674 ± 36 cm^{-1}
	B_4	−650	-699 ± 45 cm^{-1}	-765 ± 61 cm^{-1}
	B_6	−920	-949 ± 61 cm^{-1}	-978 ± 35 cm^{-1}

[a]The experimental values are from this work and Ref. 2.

attributed to roughly equal contributions from the fact that we ignored the splitting of the $J=5$ manifold and the perturbative effect of the $J=6$ manifold, as well as the fact that $B^M_{4,6}$ were restricted to cubic values.

In conclusion, therefore, we see that this simple model gives surprisingly good agreement with all the existing spectroscopic data. Indeed, further refinement of the calculation— for example, by including the $J=6$ manifold—is, in the opinion of the present authors, not justified by the accuracy of the available data. Also, in view of the agreement between our values of B_4 and B_6 and those of Finkman *et al.*[13] for $NdAlO_3$, it seems that these numbers should be sufficiently reliable to warrant comparison with a first-principles CEF calculation for a rare-earth ion in 12-fold cubic O^{2-} coordination. Such a calculation would, in light of these results, be a worthwhile contribution. Finally, it should be pointed out that the assumption used here, namely, that the fourth- and sixth-order CEF parameters are unaffected by the distortion of the perovskite lattice, may well prove applicable to other similar systems, even those involving different distortions. In fact, it is probably a useful first approach to any such problem.

ACKNOWLEDGMENTS

The authors would like to acknowledge the help of Brage Golding in attempting to measure the piezoelectric constant, as well as helpful conversations with Paul Fleury and J. K. Kjems.

APPENDIX

We are concerned in this Appendix with the $l=2$ components of the crystal field at the Pr sites due to the atomic motions which occur in $PrAlO_3$. These effects can in general be represented by a traceless symmetric second-rank tensor which we shall call B_{ij}. For the moment we shall drop the requirement of tracelessness. In cubic symmetry B_{ij} must have the form $B\delta_{ij}$. If the lattice is strained, then to first order in the strain $\hat{B}_{ij} \equiv B_{ij} - B\delta_{ij}$ is given by

$$\hat{B}_{ij} = C^S_{ijkl}\epsilon_{kl} . \qquad \text{(A1a)}$$

Here we are using, for notational convenience, the slightly unconventional definition $\epsilon_{ij} = \frac{1}{2}[(\partial u_i/\partial x_i) + (\partial u_i/\partial x_i)]$ for all i, j where $\vec{u}$ is the displacement. The more conventional definition does not have the factor $\frac{1}{2}$ when $i \neq j$.

Since C^S_{ijkl} is a constitutive tensor, it must satisfy the requirements of cubic symmetry:

$$C^S_{ijkl} = C^S\delta_{ij}\delta_{kl} + B^S(\delta_{ijkl} - \tfrac{1}{3}\delta_{ij}\delta_{kl}) + \tfrac{1}{2}A^S(\delta_{ik}\delta_{jl} + \delta_{il}\delta_{jk} - 2\delta_{ijkl}), \quad \text{(A1b)}$$

where δ_{ijkl} vanishes unless all indices are equal, when it is 1. There are three independent coefficients because the symmetric tensors B_{ij} and ϵ_{kl} decompose into three irreducible representations, A_1, E_g, T_{2g}, under the cubic group, corresponding, respectively, to C^S, B^S, A^S; this is entirely analogous to the fact that there are three independent elastic moduli in cubic materials.

Likewise, if instead of a strain we produce a displacement of the atoms corresponding to a threefold degenerate optic mode at Γ or R, we obtain similar expressions with ϵ_{ij} replaced by $\omega_i\omega_j$ where the ω_i $(i=1,2,3)$ are the generalized coordinates corresponding to the displacements. In the present case ω_i represents a rotation of the O's about the i axis through the Al's. In this case, we use superscript R instead of S. In expressions valid for either case, we will omit the superscript. In Sec. II we use the notation $Q_i = Q\cos\theta_i$, $Q^2 = \sum Q_i^2$, $B_2 = \frac{1}{3}B$, $\alpha = -A/B$.

This is all that symmetry can tell us. It is, however, of some value to see that the introduction of additional assumptions leads to some additional relations between the coefficients. Before introducing these assumptions, we shall develop the theory in terms of atomic displacements.

For the case of uniform strain we can write

$$\hat{B}_{ij} = \sum_{\vec{R},k,l} [B_{ij;k}(\vec{R})R_l]\epsilon_{kl}, \quad \text{(A2)}$$

where $B_{ij;k}$ is a partial derivative of B_{ij} with respect to the displacement of the atom at $\vec{R}$. {In general, when a crystal is strained, the atoms may suffer displacement $\hat{u}$, which has the periodicity of the lattice, in addition to the pure strain displacement $\vec{\epsilon}\cdot\vec{R}$. Here we are assuming that no such displacements occur. This is equivalent to the assumption that there are no Raman-active optic modes. If such modes existed they would invalidate the relation to be obtained below [(A8)]. For the perovskite structure such modes do not exist, though they do for, say, garnet.}

For the second-order effect due to the optic mode Q_i we have

$$\hat{B}_{ij} = \sum [B_{ij;mn}(R)d_{mk}(R)d_{nl}(R)]Q_kQ_l, \quad \text{(A3)}$$

where d_{mk} is the motion of R in the m direction produced by a unit displacement of the k mode and $B_{ij;mn}$ is the second derivative of B_{ij} due to motion at R.

In either case, we represent the quantity in brackets by $A_{ijkl}(R)$, which is symmetric under the interchange of i and j or of k and l.

Let us consider a set S of neighbors of the central ion—where we are calculating B_{ij}. This set consists of sites transformed into each other by the operations of the cubic point group. For any member R of this set

$$A_{ijkl} = \sum_{i',j',k',l'} D_{ii'}D_{jj'}\bar{D}_{kk'}\bar{D}_{ll'}A_{i'j'k'l'}(R_0), \quad \text{(A4)}$$

where R_0 is a fixed member of the set. Here $D_{ii'}$ is an element of the matrix representing the transformation of a vector by an operator belonging to the cubic point group, which takes $\vec{R}_0$ to $\vec{R}$. If we are discussing strain, $\bar{D}_{mm'} = D_{mm'}$; otherwise, $\bar{D}$ is the matrix representing the effect of the same operation applied to the Q's, the bar indicating that the Q's may belong to a different representation.

We can sum R over the set by summing the right-hand side over the g operations of the cubic group and dividing by the order $g(R_0)$ of the group under which R_0 is invariant. Using standard methods, the sum of the product of D's is found to be

$$N(S)\sum_{\alpha,\mu,\nu}\frac{1}{d_\alpha} \times B(ij,\alpha\mu)B^+(\alpha\mu,kl)B(k'l',\alpha\nu)B^+(\alpha\nu,i'j'), \quad \text{(A5)}$$

where $B(ij,\alpha\mu)$ is the unitary matrix taking the index pair i,j into component μ of the irreducible representation α of dimension d_α. The same matrix applies for k,l even if Q_k belongs to a different irreducible representation, provided it is three dimensional. $N(S) \equiv g/g(R_0)$ is the number of sites in the set S.

The following identities are easily established. The values 1, 3, 5 for α refer to Bethe's notation Γ_α for the irreducible representations, $\Gamma_1 \sim A_1$, $\Gamma_3 \sim E_g$, $\Gamma_5 \sim T_{2g}$:

$$A(ij,1)B^+(1,kl) = \tfrac{1}{3}\delta_{ij}\delta_{kl}, \quad d_1 = 1$$

$$\sum_{\mu=1,2} A(ij,3\mu)B^+(3\mu,kl) = (\delta_{ijkl} - \tfrac{1}{3}\delta_{ij}\delta_{kl}), \quad d_3 = 2 \quad \text{(A6)}$$

$$\sum_{\mu=1}^{3} A(ij,5\mu)B^+(5\mu,kl) = \tfrac{1}{2}(\delta_{ik}\delta_{jl} + \delta_{il}\delta_{jk} - 2\delta_{ijkl}), \quad d_5 = 3.$$

The contribution of the atoms of set S to C_{ijkl} then becomes

$$N(S)\left\{\tfrac{1}{9}\delta_{ij}\delta_{kl}\sum_{st}A_{sstt} + \tfrac{1}{2}(\delta_{ijkl} - \tfrac{1}{3}\delta_{ij}\delta_{kl})\left[\sum_s A_{ssss} - \frac{1}{3}\sum_{st}A_{sstt}\right] + \tfrac{1}{6}(\delta_{ik}\delta_{jl} + \delta_{il}\delta_{jl} - 2\delta_{ijkl})\left(\sum_{st}A_{stst} - 2\sum_s A_{ssss}\right)\right\}. \quad \text{(A7)}$$

In general, the expression in braces contains three independent sums, $\sum A_{ssss}$, $\sum A_{sstt}$, and $\sum A_{stst}$, corresponding, though not one-to-one, with independent A, B, C in Eq. (A1). If $B_{ij}(R)$ is a field gradient produced by a charge density which does not extend to the origin, $\sum_i B_{ii,k}$ and $\sum_i B_{ii;kl}$ vanish and so must $\sum A_{sstt}$, but A and B remain independent.

If, however, we add the assumption that the charge distributions at the sites R move rigidly, $B_{ij;k}$ and $B_{ij;kl}$ become third and fourth derivatives, symmetric in all interchanges of indices, and we shall omit the semicolon. For the strain case, then, $\sum A_{stst} = \sum B_{sts} R_t$ vanishes like $\sum A_{sstt}$, and we have, on summing over all the shells S of neighbors,

$$\hat{B}_{ij} = \sum_{S,k,l} N(S) M[(\delta_{ijkl} - \tfrac{1}{3}\delta_{ij}\delta_{kl}) - \tfrac{1}{3}(\delta_{ik}\delta_{jl} + \delta_{il}\delta_{jk} - 2\delta_{ijkl})]\epsilon_{kl}, \quad \text{(A8)}$$

$$M = \frac{1}{2}\sum_s B_{sss} R_s.$$

In terms of Eq. (A1), $C^S = 0$, $A^S = -\frac{2}{3}B^S$.

The optic-mode case is somewhat more complicated since

$$A_{ijkl} = B_{ijmn} d_{mk} d_{nl} \quad \text{(A9)}$$

and, in general, there will be no relations among A, B, C. On the other hand, there are some special cases when simple relations are found, of which we will mention three.

First, for a simple optically active mode in a zinc-blende or rocksalt structure, $d_{kl} \propto \delta_{kl}$ so that $A_{ijkl} = B_{ijkl}$ and we obtain the same result as for the strain case with $B_{sss} R_s$ replaced by B_{ssss}.

In $PrAlO_3$ there are two modes, similar to the one just discussed, in which the Pr, Al, and O sublattice individually move rigidly—but not together, as in the uniform translation. They are, however, coupled harmonically to another mode in which the O's have no net motion. For the resulting eigenmodes no simple relation exists between A and B.

On the other hand, for the two triply degenerate R-point modes involving O's, the situation does simplify. We choose for R_0 an oxygen whose nearest-neighbor aluminums are in the z direction. In the case of the staggered-rotation mode, $d_{kl}(R_0) = \frac{1}{2}a\epsilon_{3kl}$, where a is the perovskite lattice parameter and ϵ_{ijk} is the standard antisymmetric tensor. For the other mode, which looks like a shear of the oxygen octahedra, $d_{kl} = \frac{1}{2}a\,|\,\epsilon_{3kl}\,|$. In the first case we again obtain Eq. (A8) with $M = (\frac{1}{2}a)^2 B_{1122}$. In the second case we obtain the same thing, except that the sign between the pairs of parentheses is a plus.

We note in passing that these relations are valid not only for the point-charge model, but for any set of charge distributions at the various sites compatible with over-all cubic symmetry. Thus the oxygens could have quadrupole moments and the aluminums and praseodymiums hexadecapole moments.

Should the charge distributions extend to the origin, $C \neq 0$ and for the cases of strain and staggered rotation $A^S = -\frac{2}{3}B^S + 2C^S$ and $A^R = -\frac{2}{3}B^R - C^R$, respectively.

Now we shall evaluate M for the strain and rotation-mode cases in the point-charge model (PCM). We have

$$B_{ijk} = Ze\left(-\frac{15R_iR_jR_k}{R^7} + \frac{3(\delta_{ij}R_k + \delta_{ij}R_j + \delta_{ik}R_i)}{R^5}\right),$$

$$B_{ijkl} = Ze\left(\frac{105R_iR_jR_kR_l}{R^9} - \frac{15(R_iR_j\delta_{kl} + \cdots)}{R^7} + \frac{3(\delta_{ij}\delta_{kl} + \cdots)}{R^7}\right), \quad \text{(A10)}$$

where $+\cdots$ indicates that all distinct terms obtained by permuting i, j, k, l are to be added, and Ze is the charge of the ion at $\vec{R}$. Thus we find

$$\sum_s B_{sss} R_s = -Ze\frac{15\sum R_i^4 - 9R^4}{R^7} = -Ze\left(\frac{2}{a}\right)^3 \frac{15\sum n_i^4 - 9\sum n_i^2}{(\sum n_i^2)^{7/2}} \equiv -Ze\left(\frac{2}{a}\right)^3 f_1, \quad \text{(A11)}$$

$$B_{1122} = Ze\left(\frac{2}{a}\right)^5 \frac{105n_1^2n_2^2 + 15n_3^2\sum n_i^2 - 12\sum n_i^2)^2}{(\sum n_i^2)^{9/2}} \equiv Ze\left(\frac{2}{a}\right)^5 f_2, \quad \text{(A12)}$$

where $n_i = 2R_i/a$.

Finally then, we obtain for the case of strain

$$B^S = \frac{e}{2}\left(\frac{2}{a}\right)^3 \sum_{\text{neighbor}} Zf_1 \quad \text{(A13)}$$

and for the case of the rotation mode

$$B^R = 24e\left(\frac{2}{a}\right)^3 \sum_{n_i}{}' f_2, \quad \text{(A14)}$$

where the primed sum is to be taken over oxygen sites of the form n_1, n_2 odd and positive, n_3 even and positive or negative. The factor 24 consists of $2 = Z$ and 12 to account for oxygen sites not included in the sum.

The sum in (A14) converges fairly rapidly, nearest neighbors contributing 2.19, while inclusion of neighbors out to $\sum n_i^2 = 58$ indicates a value between 2.520 and 2.521; we shall use 2.52. The sum in (A13) oscillates significantly out to the same value of $\sum n_i^2$ and suggests a value of $13.5 \pm .3$. The contributions of the O, Al, and Pr nearest neighbors are 18, -18.5, and 13.5, respectively, with a sum of 13.0. We shall use 13.5.

Thus we take

$$B^S = -6.75\, e(2/a)^3,$$
$$B_R = 60.5\, e(2/a)^3, \qquad \text{(A15)}$$
$$A^{S,R} = -\tfrac{2}{3} B^{S,R}.$$

Leaving the PCM for a while, we have four parameters A^S, B^S, A^R, and B^R relating the field gradient to the distortion of the structure from cubic. Using the measured Q's, ϵ's, and spectroscopic data for the tetragonal, orthorhombic, and trigonal phases, we could combine the parameters linearly to obtain as new parameters the four independent field gradients in these phases, two for the orthorhombic and one each for the others. These parameters could then be evaluated by a least-squares fit and the original parameters evaluated. This would seem to be overinterpreting the data.

A more attractive approach is to follow Birgeneau *et al.* in arguing that the strain should be expressible in terms of the Q's, by a relation of the form

$$\epsilon_{ij} = \sum_{kl} D_{ijkl} Q_k Q_l$$

analogous to (A1). We could then obtain a tensor

$$C_{ijkl} \equiv C^R_{ijkl} + \sum_{mn} C^S_{ijmn} D_{mnkl}$$

relating $\hat{B}_{ij}$ to the Q's.

Unfortunately, there is no guarantee that any of these tensors are temperature independent and the experimental data indicate that D_{ikjl} is not. From the data of Birgeneau *et al.*[2] it can be seen that the ratio $\delta_3 \equiv (\epsilon_{33} - \frac{1}{3}\epsilon)/(Q_3^2 - \frac{1}{3}Q^2)$ is, within the accuracy of the data, 0.5 in the tetragonal phase and 0.25 in the orthorhombic phase. This discrepancy is outside the quoted error estimates. Likewise, from the rhombohedral and orthorhombic phases, we find values for $\delta_5 \equiv (\epsilon_{12}/Q_1 Q_2)$ of -0.29 and -0.22, respectively, with values of -0.25 to -0.26 being within the error estimates for both phases.

These discrepancies, particularly in δ_3, mean that one cannot actually express the strain as a quadratic in the Q's, at least with temperature-independent coefficients. Fortunately, the strain terms appear, in the PCM anyway, to be rather small. Defining $A = A^R + A^S\delta_5$, $B = B^R + B^S\delta_3$, using PCM values for A's and B's and the experimental δ's, we obtain the following results:

$$B = (58.0 \pm 1) \times e(2/a)^3,$$
$$A = -(41.5 \pm 0.14) \times e(2/a)^3 \quad \text{(PCM)}, \qquad \text{(A16)}$$
$$-A/B = 0.72 \pm 0.1.$$

The mean values here are obtained by using the averages of the values quoted above for δ_3 and δ_5, while the "errors" for A and B indicate the changes which would be produced by using the values of the δ's obtained from individual phases. The "error" for A/B represents the square root of the sum of the squares of the relative "errors" in A and B.

On the basis of these numbers we feel that it is more reasonable to treat A and B as fitting parameters in our calculations. The temperature variation suggested by (A16) would produce changes in the crystal-field levels well within the experimental and computational uncertainties.

While the foregoing computations were based on the PCM, it was used only for guidance and we are not surprised that the values of α obtained by fitting the data are significantly smaller.

It should be remarked that in the orthorhombic and monoclinic phases the Pr atoms themselves may be displaced from their perovskite sites, their displacement corresponding to another R-point phonon of different symmetry from the rotation mode. In terms of the model used here for the distortion, it should be of at least third order in Q, and by interaction with the Q's could produce terms in $\hat{B}_{ij}$ of fourth and higher order in Q. It is consistent with our approach to neglect this effect, which in any case has not been measured accurately.

As a final remark, we would like to comment on the obvious analogy between the relation $A^S = -\frac{2}{3}B^S + 2C^S$ and the Cauchy relation $C_{12} = C_{44}$ between the elastic moduli. Indeed, if we reexpress the elastic moduli in terms of $\bar{A}$, $\bar{B}$, $\bar{C}$ as in (A1b), the Cauchy relation takes exactly the same form. The latter is valid if the atoms interact by central forces and if they are situated at sites for which $\hat{u}$, mentioned after (A2), vanishes. The second requirement is thus the same for our relation and Cauchy's, while the latter is more demanding in requiring central forces. The reason for this is as follows. For our problem $\sum A_{ststt} = \sum A_{sstt}$ provided B_{ijk} is symmetric in all indices. For the elastic moduli,

$$A_{ijkl} = \tfrac{1}{4}(R_i V_{jk} R_l + R_j V_{ik} R_l + R_i V_{jk} R_k + R_j V_{il} R_k)$$

and

$$\sum A_{sstt} = \sum R_i V_{ij} R_j$$
$$\neq \frac{1}{2}\left(\sum R_i V_{ij} R_j + R^2 \sum V_{ij}\right) = \sum A_{ststt},$$

just because V_{ij} is symmetric. To establish the Cauchy relations requires not only central forces, but use of the fact that the stress is initially zero.

For lower symmetries, the situation is more complicated and we add only that for triclinic symmetry, the symmetry of B_{ijk} in all indices does

not imply that $A_{ijkl}=A_{klij}$, but does imply that $(A_{ijkl}+A_{klij})$, being already symmetric in (ij) and in (kl), is symmetric in all indices.

Note added in proof. After submission of this manuscript a polarized absorption experiment on $PrAlO_3$ was completed by M. Sturge *et al.* (private communication). Since their crystal was monodomain, they were able to substantiate unambiguously the symmetry assignments for the orthorhombic (C_{2v}) phase given above.

[1]R. J. Birgeneau, J. K. Kjems, G. Shirane, and L. G. Van Uitert, Phys. Rev. B 15, 1300 (1974).

[2]R. T. Harley, W. Hayes, A. M. Perry, and. S. R. P. Smith, J. Phys. C (Lond.) 6, 2382 (1973); also, S. Geller and P. M. Racah, Phys. Rev. B 2, 1167 (1970).

[3]P. A. Fleury, P. D. Lazay, and L. G. Van Uitert, Phys. Rev. Lett. 33, 492 (1974). This transition shows negligible effects on the observable crystal-field electronic levels. Hence it is ignored in the remainder of the paper.

[4]R. J. Elliott, R. T. Harley, W. Hayes, and. S. R. P. Smith, Proc. R. Soc. Lond. A328, 217 (1972).

[5]E. Cohen, M. D. Sturge, R. J. Birgeneau, E. I. Blount, L. G. Van Uitert, and J. K. Kjems, Phys. Rev. Lett. 32, 232 (1974).

[6]E. Ryder (unpublished).

[7]R. D. Burbank, J. Appl. Cryst. 3, 112 (1970).

[8]A search for piezoelectric activity in $PrAlO_3$ [B. Golding (private communication)] has yielded a null result. If nonzero, the piezoelectric coefficient must be at least 50 times weaker than that of quartz.

[9]K. R. Lea, M. J. M. Leask, and W. P. Wolf, J. Phys. Chem. Solids 23, 1381 (1962).

[10]A. Abragam and B. Bleaney, *Electron Paramagnetic Resonance of Transition Ions* (Clarendon, Oxford, England, 1970), p. 677 and Appendix B. Their equation (16.35) lacks a factor of $[(J+1)^2-J_z^2]^{1/2}$.

[11]These data, directly available for only seven of the nine levels, were obtained from Ref. 2 (see Fig. 2). The lower A_2 value was estimated by extrapolation from the monoclinic phase. The B_2 levels were "identified" by the results of the calculations.

[12]Existing computer programs made this approach significantly easier to use than a fit to all the data simultaneously. The fact that both procedures gave similar parameters and accuracy within that expected not only acted as a test of the internal consistency of the model but also indicated that the additional programming effort involved in an over-all fit would not be justified.

[13]E. Finkman, E. Cohen, and L. G. Van Uitert, in *Proceedings of the Second International Conference on Light Scattering in Solids*, edited by M. Balkanski (Flammarion, Paris, 1971), p. 369; Phys. Rev. B 7, 2899 (1973).